CCFE
CULHAM CENTRE FOR FUSION ENERGY

UK Atomic Energy Authority

UKAEA-CCFE-CP(23)58

J. Northall, M. Darby, A. Cooper, ; A. Hollingsworth,
A. Wohlers, Y. Zayachuk

Synthesis of Erbium Deuteride by Ion Beam Implantation

Synthesis of Erbium Deuteride by Ion Beam Implantation

J. Northall, M. Darby, A. Cooper, ; A. Hollingsworth, A. Wohlers, Y. Zayachuk

This paper has been submitted to
13th International Tritium Science and Technology Conference, Radisson Blu Hotel, Bucharest, Romania, 16 - 21 October 2022

Synthesis of Erbium Deuterides via Deuterium Ion Implantation into Erbium Thin Films

J. Northall[1*] (0000-0003-3919-4116), M. S. B. Darby[1], A. Cooper[2] (0000-0003-4496-0786), A. Hollingsworth[2] (0000-0002-2251-506X), Y. Zayachuk[2], A. Wohlers[2], A. Simons[1], and H. Smith[2]

1) AWE, Aldermaston, Reading, RG7 4PR, United Kingdom

2) UKAEA, Culham Science Centre, Abingdon, OX14 3DB, United Kingdom

*Electronic mail: jon.northall@awe.co.uk

Synthesis of Erbium Deuterides via Deuterium Ion Implantation into Erbium Thin Films

An experimental study of a synthesis technique in which deuterium ions are implanted into thin films of erbium to form erbium deuterides is presented. Results from thermal desorption spectroscopy indicate the synthesis of multiple hydride phases has occurred, including ErD_3 and ErD_2. The findings also indicate that, for erbium deuteride synthesis via ion beam bombardment, elevated substrate temperatures are not required to promote deuterium uptake in the film. Stoichiometries of up to $ErD_{0.21}$ were achieved for a 400 nm film exposed to a 1000 eV ion beam for 5 hours at a deuterium ion fluence of 3.6×10^{22} m^{-2}. Over the tested experimental conditions, deuterium uptake was found to scale linearly with deuterium ion fluence and ion energy. The presence of deuterium in the film was confirmed by secondary ion mass spectrometry.

Keywords: Deuterium, Erbium, Ion implantation and Materials science.

I. INTRODUCTION

There are many transition and rare earth metals, as well as some actinides, which are suitable for the long-term storage of hydrogen due to their high volumetric hydrogen density and high thermal stability. Metals such as magnesium, titanium, vanadium, zirconium, lanthanum and uranium have been demonstrated to uptake significant quantities of hydrogen.[1-6]

The well-established method for forming metal hydrides is to expose the metal to molecular hydrogen gas at elevated temperatures. In this technique, the gas is absorbed onto the surface of the metal and the hydrogen atoms diffuse throughout the metal to form a metal hydride phase.[7-8] Typically, thermal treatment is required to prepare the surface of the metal prior to hydrogen exposure and the temperature and pressure of the loading conditions affects the phase and composition of the metal hydride formed.

Understanding the effects of energetic ions on materials is essential for the design of fusion energy systems.[9-15] In previous reports the effects of plasma environments on materials are predicted by exposing materials to ion beams in a controlled experiment. However, another application of such a system is the synthesis of new materials by incorporating the incident ions into the material to form new compounds. Several studies have been reported on this topic with various materials such as zirconium, copper, titanium, magnesium, tungsten, palladium, nickel and vanadium.[16-23]

A number of authors report ion-induced modification of the material's surface following ion beam implantation.[16-19,22,24] Reports suggests that lattice defects caused by ion beam exposure result in a quantitative increase in the hydrogen uptake in the material. Also of note is that, for some materials, increased levels of ion damage have been shown to reduce the rate of hydrogen outgassing.[24]

A comparison of hydriding and non-hydriding materials has been reported which studied the dynamics of non-equilibrium conditions of ion implantation compared with conventional gas loading.[18] In titanium, which forms hydrides, the deuterium migrated to the surface and formed a saturated layer which diffused into the sample. This contrasted with copper, which does not form hydrides, in which it was found that the distribution of deuterium was centred on the implantation depth of ions.

Erbium hydride is a suitable material for the long-term storage of hydrogen due to its high hydrogen sorption capacity and its high thermal stability.[25-26] However, an oxide layer is readily formed on the surface which inhibits the uptake of hydrogen. Therefore, gas loading of erbium is often conducted at elevated temperatures in order to achieve high gas-to-metal ratios.[7,27-28] Gas-to-metal ratios of 2:1 (corresponding to ErD_2) or greater are typically desirable for hydrogen storage purposes due to the thermal stability of this compound. The presence of surface oxide itself has been suggested to cause the hydrogen desorption peak to occur at higher temperatures and therefore improve thermal stability.[29]

This work assesses the feasibility of loading erbium films with deuterium by means of ion beam implantation with a longer-term goal to load samples with tritium. Samples were implanted using the Device for Exposure to Low-energy Plasma of Hydrogen Isotopes (DELPHI) facility within the Hydrogen-3 Advanced Technology (H3AT) department at UKAEA. This ion exposure system is used to investigate the interaction of hydrogen isotopes with materials by using low energy plasmas.

II. EXPERIMENTAL

II.A. Sample Manufacture and Preparation

Thin films of erbium with a nominal thickness of 400 nm were deposited onto molybdenum substrates using an electron beam physical vapour deposition system which was cryo-pumped to a base pressure of less than 10^{-8} mbar. Prior to coating, the substrates were

cleaned using a chemical etch to remove the surface contaminants. The films were deposited at a substrate temperature of 500 °C under a vacuum of less than 10^{-8} mbar and at a deposition rate of 0.4 nm/s. The deposition rate was measured in-situ using a quartz crystal microbalance. Following deposition, samples were transferred to a storage cabinet filled with a nitrogen atmosphere. During transportation, the samples were stored in air and, on arrival at UKAEA, were transferred to a desiccator and stored under vacuum at less than 0.1 mbar.

II.B. Ion Exposure System

The ion exposure system is a custom ultra-high vacuum (UHV) implantation system and its design has previously been reported in detail.[24] During operation, low energy ions are generated in a boron nitride plasma chamber within a modified version of a commercially available SPECS PCS-ECR microwave ion source. The plasma source produces a 2.45GHz radially symmetric microwave field which provides the main heating source for the hydrogen plasma. Hydrogen ions are extracted and accelerated from the plasma via high voltage (HV) ion optics and are guided to the sample. The sample is mounted onto a sample holder plate located approximately 60 mm from the aperture of the ion source. The sample stage incorporates a cooling and heating system which controls the temperature between 4 °C and 450 °C. Samples are introduced into the system via a sample loading chamber and load-lock system which allows sample handling under vacuum.

Prior to ion beam exposure, some samples were held under vacuum within the chamber for a duration of either 30 minutes or 1 hour at a temperature of 450 °C and 300 °C, respectively. Samples were then exposed to a deuterium ion beam with an ion energy of between 200 eV and 1000 eV for a duration of up to 5.5 hours. The samples were exposed at a substrate temperature of ambient temperature or 250 °C. The isotopic composition of the gas injected into the plasma source has been measured previously to be 99.8 mol% deuterium, 0.2 mol% protium, and the deuterium ion mass and charge incident on the sample

is assumed to be 97 mol% D_3^+, 2 mol% D_2^+ and 1 mol% D^+ based on findings from a similar system.[30] The ion current incident on the sample stage during exposure was measured with a Keithley 2100 digital multimeter for each sample and used to determine the deuterium ion flux and total fluence. The plasma performance and plasma stability were monitored during exposure through a Kodial glass viewport by a photodiode power sensor (Thorlabs S121C) fixed to the outside of the plasma chamber. A spectrometer (Hamamatsu C10083CAH) was also used to monitor the plasma purity. After each exposure, the plasma was turned off and the sample was extracted via the load-lock system before being sent for further analysis.

II.C. Thermal Desorption Spectroscopy

Thermal Desorption Spectroscopy (TDS) measurements of samples was conducted within an evacuated vacuum chamber using a modified Hiden Analytical TPD Workstation Type 640100. During transfer from the ion exposure system to the TDS system, samples were exposed to ambient air. The time between the end of ion exposure and beginning of TDS measurement was less than 20 hours. During the TDS process, the samples were heated at a rate of 10 °C/min from ambient temperature to 750 °C under vacuum at 10^{-9} mbar and were held at 750 °C for 1 hour. The pressure in the system increases slightly during heating due to the sample outgassing but typically does not exceed $7x10^{-8}$ mbar. The masses of the desorbed species were measured using a line-of-sight quadrupole mass spectrometer. Mass-to-charge ratios (m/z) were monitored specifically for the presence of the molecular ion peak of H_2, HD and D_2. Signals from m/z ratios of 18 (H_2O), 20 (D_2O, Ne), 28 (N_2, CO_2), 32 (O_2) and 44 (CO_2) were also captured to monitor irregularities that may occur during analysis.

For each sample, a background TDS measurement was made and subtracted from the experimental data for each sample. Release signals of deuterium-containing molecules (H_2, HD and D_2) were quantified using calibrated hydrogen and deuterium leaks. The calibration factor for the HD signal was determined by averaging the calibration factors for H_2 and D_2.

The total amount of deuterium released was calculated from the time-integrated molecular release signals.

In this paper, we introduce two figures of merit (FOM) which are used in the analysis of the TDS data. The first is the deuterium retention, which is a measure of the total number of deuterium atoms desorbed from the sample divided by the exposed area of the sample. The total number of deuterium atoms absorbed was calculated by numerical integration of the TDS data. Unexposed samples were found to contain negligible quantities of deuterium. In addition, heating of an exposed sample to 1000 °C was not found to desorb significantly more deuterium than heating to 750 °C. Based on this, it is assumed for all samples that there is a negligible amount of deuterium either pre-existing in the sample or retained after heating to 750 °C during the TDS analysis.

The second FOM is the deuterium absorption yield which is a measure of the fraction of absorbed deuterium per incident deuterium atom. Both these figures of merit account for the differences in sample's area, but only the deuterium absorption yield accounts for variations in the ion fluence for each experiment. The deuterium retention value, however, requires fewer inputs as it does not require measurement of the ion flux and directly gives an indication of the quantity of deuterium desorbed. Together, these figures of merit provide a way to compare experiments with different experimental conditions and to account for variations in sample size and ion flux.

II.D. Secondary Ion Mass Spectrometry

Secondary ion mass spectrometry (SIMS) analysis of exposed and unexposed samples was conducted using a Cameca IMS Model 4f secondary ion mass spectrometer. A focused 14.5 keV $^{133}Cs^{+}$ primary ion beam was rastered over a 200 x 200 μm area and secondary ions with a mass to charge ratio (m/z) of 1, 2, 18, 98 and 166 were monitored. Electron multiplier (EM) detection was configured with a mass resolution of approximately 1600 to allow

separation of $^{2}D^{-}$ from any $^{1}H_{2}^{-}$ ions at m/z 2 and $^{18}O^{-}$ ions, from any $(^{16}O + {}^{2}D)^{-}$ and $(^{16}O + {}^{1}H_{2})^{-}$ molecular interferences, at m/z 18. $^{16}O^{-}$ was not monitored as its relative intensity was significantly higher than the other ion signals, and therefore above the detection limit of the EM detector, for the analysis conditions used. The other m/z signals monitored were assigned to $^{1}H^{-}$, $^{98}Mo^{-}$ and $^{166}Er^{-}$.

III. RESULTS AND DISCUSSION

III.A. Thermal Desorption Spectroscopy

Thermal desorption spectra consisted of three distinct peaks with average peak positions of 270 °C, 450 °C and 710 °C (Figure 1). Literature suggests that the peaks may be due to the decomposition of ErD_3 (hexagonal close packed erbium with deuterium in octahedral sites), $ErD_{2(oct)}$ (face centre cubic erbium with deuterium in octahedral sites) and $ErD_{2(tet)}$ (face centre cubic erbium with deuterium in tetrahedral sites), respectively.[8,31-33] For all samples, the majority of deuterium was evolved from the decomposition of $ErD_{2(tet)}$. Peaks for ErD_3 and $ErD_{2(tet)}$ are consistent with the peaks reported in the literature for conventional gas loading.[8,31-33]

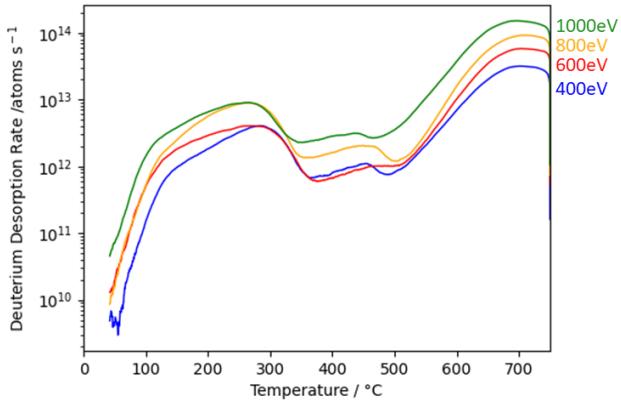

Figure 1. TDS spectra for a selection of samples exposed to a deuterium ion beam at varying ion energies. The y-axis is plotted on a log scale

The peak at approximately 450 °C is less well-characterised in the literature. Early work on the erbium-deuterium system observed a peak at 350 °C and inspection of the data indicates there may also be a peak at approximately 450 °C.[33] These peaks were not explained conclusively. It has been shown that deuterium can reside in the octahedral sites of the erbium dideuteride lattice with a percentage of between 2 and 15 %.[34] However, the tetrahedral sites were found to have 100 % deuterium occupancy for all measured samples and were thus identified to be heavily preferred. Later work postulated that a peak observed at 450 °C may be due to desorption of deuterium from octahedral sites and further work found that the fraction of hydrogen in the octahedral sites was reduced by heating to temperatures above 400 °C under UHV.[34-35] Therefore, it is proposed that this peak is due to the release of deuterium from the octahedral sites in the dideuteride lattice.

The deuterium retention for all samples was found to vary by nearly two orders of magnitude from 3.19×10^{19} m^{-2} up to 2.70×10^{21} m^{-2}. Total deuterium retention was found to be highest for the samples exposed at higher ion energy with ion energies of 1000, 800 and 600 eV yielding average deuterium retention values of 2.70×10^{21} m^{-2}, 1.69×10^{21} m^{-2} and 1.10×10^{21} m^{-2}, respectively. It should be noted that increasing the ion energy (i.e. accelerating voltage) increases the ion flux (as predicted by the Child-Langmuir law) due to the ion source configuration. Therefore, it was necessary to correct for this effect in later sections by calculating the deuterium absorption yield.

The ratio of deuterium to erbium atoms was calculated assuming a homogenous distribution of retained deuterium throughout a nominally 400 nm thick erbium film. The highest D:Er ratio obtained was 0.207:1, which is lower than would be expected for the formation of pure ErD_2 and ErD_3 phases (2:1 or 3:1).

Figure 2 shows the effect of ion energy on the deuterium absorption yield. The data indicate that for these exposure conditions between 1 % and 8 % of deuterium ions incident

on the sample are retained in the film. As might be expected, an increase in the deuterium ion energy was found to lead to an increase in the absorption yield. The correlation between deuterium desorption yield and ion energy was found to be approximately linear over these exposure conditions.

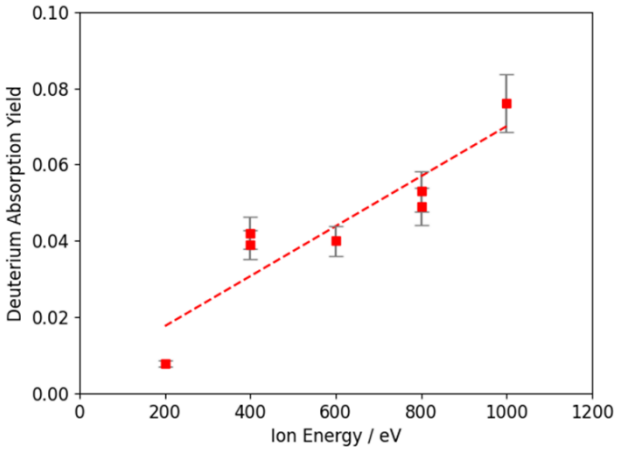

Figure 2. Plot of deuterium absorption yield against ion energy. A linear trendline has been fitted to the data

Table I lists deuterium absorption yield values at different substrate temperatures for samples exposed to an ion energy of 400 eV for 5 hours with no thermal pre-treatment. It was found that there was no appreciable increase in deuterium absorption yield for a film at a temperature of 250 °C compared to ambient temperature. For samples prepared at ambient temperature, the TDS results show that a portion of the gas was released below 250 ºC. Consequently, this gas would not be present in samples exposed at 250 °C and this would be expected to contribute to a decrease in the measured deuterium desorption.

Table I. Measured deuterium absorption yield values at different exposure temperatures

Exposure Temperature /°C	**Deuterium Absorption Yield**
22	0.042 ± 0.004
25	0.039 ± 0.004
250	0.037 ± 0.004

Table II lists the measured deuterium retention and deuterium absorption yield for samples prepared under different conditions and exposed using an ion energy of 400 eV for 5 hours. It is evident that thermal pre-treatment does not increase the deuterium uptake for the ion implantation. Indeed, deuterium absorption yield decreased with higher pre-treatment temperatures. This contrasts with the published literature for gas loading for which pre-treatment is required to remove atmospheric contaminants from the surface and to promote the diffusion of the surface oxide layer into the bulk of the sample.[7]

Table II. Measured deuterium retention values and deuterium absorption yield for thermally pre-treated samples.

Duration of Pre-treatment /hr	**Thermal Pre-treatment Conditions**	**Ion Fluence /m^{-2}**	**Deuterium Retention /m^{-2}**	**Deuterium Absorption Yield**
-	-	2.05×10^{22}	8.53×10^{20}	0.042
-	-	1.83×10^{22}	7.07×10^{20}	0.039
1	300 °C	2.42×10^{22}	8.27×10^{20}	0.034
0.5	450 °C	2.10×10^{22}	3.87×10^{20}	0.018

Simulations conducted by Mao *et al.* show that an energy of at least 1.6 eV would be required for hydrogen to penetrate the erbium oxide surface layer.[36] This suggests that the ion energies used in this work would have sufficient energy to penetrate the oxide barrier, thus eliminating the requirement for thermal pre-treatment to prepare the surface for gas absorption.

III.B. Secondary Ion Mass Spectrometry

Figure 3 compares as-measured SIMS data for an unexposed sample and a sample exposed to a deuterium ion beam. The significant difference of note is the presence of a large secondary ion signal at m/z 2 (denoted by $^{2}D^{-} + {}^{1}H_{2}^{-}$) for the exposed sample. Although the SIMS instrument was configured to resolve $^{2}D^{-}$ from any $^{1}H_{2}^{-}$ ions, only one clear ion signal was observed at m/z 2 for the exposed sample (Figure 3b). Given the very weak m/z 2 signal

in the unexposed sample (Figure 3a), we can assign the intense m/z 2 signal (Figure 3b) to deuterium and conclude that $^{1}H_2^-$ ion formation is negligible for the SIMS analysis conditions used as similarly strong $^{1}H^-$ signals are observed for both unexposed and exposed samples.

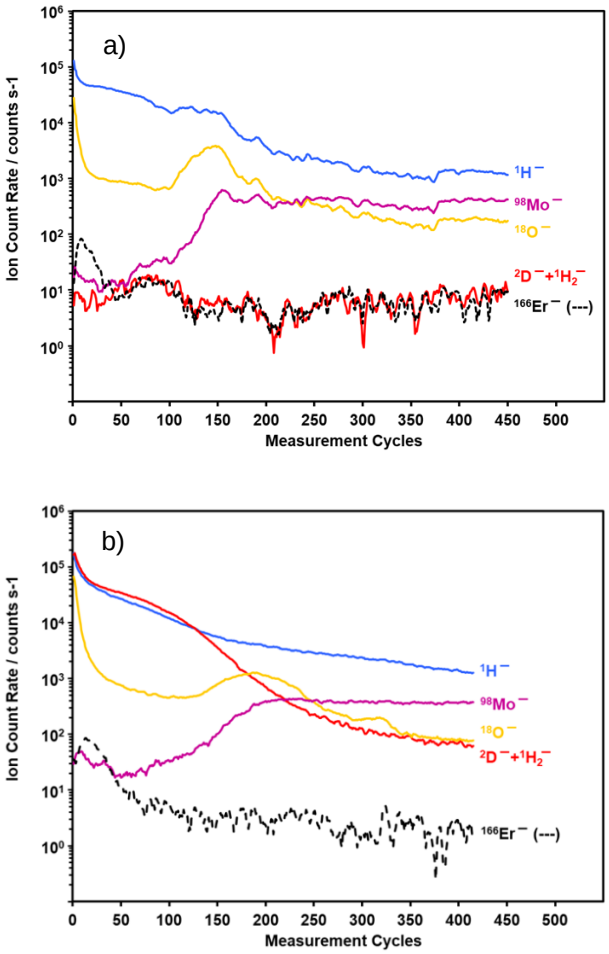

Figure 3. a) SIMS analysis of an unexposed sample. b) SIMS analysis of exposed sample: 400 eV, 5 hours, no thermal pre-treatment

With use of a $^{133}Cs^+$ primary ion beam, secondary ion yields for erbium and molybdenum are expected to be low (as compared to a $^{16}O_2^+$ beam), yet the $^{98}Mo^-$ and $^{166}Er^-$ signals, combined with $^{18}O^-$, were found to be sufficient to act as a visual guide to the observed location of hydrogen and deuterium in the erbium-molybdenum structure. An accurate depth profile is not possible with SIMS data, as the spatial distribution of measured ions might be perturbed by SIMS measurement issues such as: topographical variation of the sample surface, roughening of the sample surface and transportation of material deeper into

the sample by the primary ion beam during analysis, signal interference from outside the measured area. These issues might lead to the measured ion signals being spatially broadened and/or tailing into the erbium-molybdenum structure.

A strong surface oxygen signal and oxygen peak at the erbium-molybdenum transition, was observed in both exposed and unexposed samples, suggesting this oxygen distribution was present before exposure. The strong surface oxygen signal, combined with an increasing near-surface erbium signal, suggests an oxygen rich layer coated the erbium film. The increased oxygen signal (peak) at the erbium-molybdenum transition may be due to an oxygen rich layer present on the molybdenum substrate surface prior to erbium deposition.

Assuming the ion yields of $^{1}H^{-}$ and $^{2}D^{-}$ ions are comparable, hydrogen and deuterium are detected at similar concentrations within the exposed erbium film. The deuterium was observed throughout and tails into the molybdenum substrate. The erbium film is nominally 400 nm thick and Stopping Range of Ions In Matter (SRIM) calculations predicted a 400 eV deuterium beam should implant to a depth of 53 Å (Figure 4).[37] Given the potential SIMS signal broadening and tailing issues mentioned above, we cannot conclude that the SIMS data disagree with the SRIM calculations. Irrespective of any measurement issues, the majority of the deuterium signal was weighted toward the erbium surface.

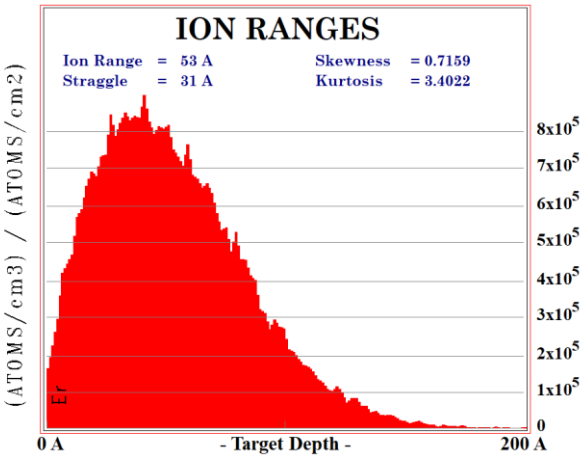

Figure 4. SRIM calculations predicting ion range for a 400 eV D_3^+ ion on an erbium film.[37]

The calculated stoichiometries suggest that deuterium migrated beyond the implantation depth, predicted by SRIM calculations. The measured deuterium retention in samples exposed to a 400 eV beam corresponded to an equivalent ErD_2 film thickness of 108 – 131 Å. This is more than double the 53 Å implantation depth predicted by SRIM calculations.

Figure 5 shows a plot of the deuterium retention for samples prepared with various deuterium ion fluences. For the samples studied, the measured deuterium retention increases with the deuterium ion fluence. It might be expected that, as ion fluence increases, the sample would eventually become saturated or reach a saturation condition under which no further deuterium accumulates in the erbium-deuterium matrix. However, the data show that saturation was not reached for the sample conditions in this study.

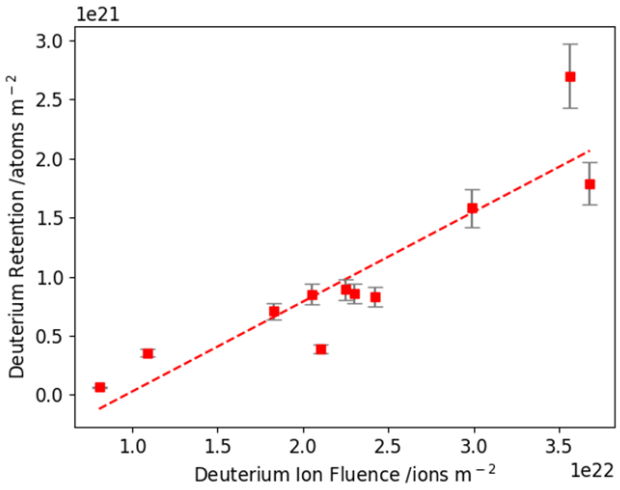

Figure 5. Deuterium retention plotted against deuterium ion fluence for all samples tested

It is of interest to increase the ion fluence further to assess what might be the maximum achievable deuterium retention via ion beam implantation. This could be achieved by utilising a higher flux ion source or increasing the exposure duration. For the experimental configuration detailed in this work, ion flux and ion energy are correlated and cannot be independently varied. Fortunately, increasing the ion energy yields both an increased ion flux

and, as detailed in this paper, an improved absorption yield. As such, utilising higher ion energies is a promising option for maximising deuterium implantation within this system. However, it should be considered that higher ion energies yield an increased likelihood of sputtering and sample damage occurring.

IV. CONCLUSIONS

This study has demonstrated a technique for deuterium loading of erbium films using a deuterium ion beam exposure system. The effects of the ion beam loading conditions on the film's composition have been investigated by TDS and SIMS. It was found that the maximum amount of deuterium loaded into the film was relatively low, corresponding to a maximum deuterium composition of $ErD_{0.21}$. Deuterium saturation in the metal matrix was not evident in the data. Elevated exposure temperatures and thermal pre-treatment did not lead to an increase in deuterium retention, which contrasts with effects of these parameters on conventional gas loading techniques.

SIMS data confirmed that deuterium was weighted towards the surface of the erbium film. The calculated stoichiometry also suggests that migration of deuterium beyond the predicted implantation depth has occurred. However, further experimental work would be required to better understand and quantify the depth profile of implanted deuterium in these samples.

Increasing exposure duration, the ion flux/fluence or ion energy all may result in higher deuterium uptake. A future study into the optimisation of the process is required to further understand the benefits of ion implantation compared to conventional gas loading techniques and to understand how this approach could be used for the production of tritium loaded samples.

V. DECLARATIONS

Funding

The authors did not receive any support from any organization for the submitted work.

Disclosure statement

The authors have no conflicts of interest to declare that are relevant to the content of this article.

Data Availability

The datasets generated during and/or analysed during the current study are available from the corresponding author on reasonable request.

VI. REFERENCES

[1] Z. SUN et al., "Enhancing Hydrogen Storage Properties of MgH_2 by Transition Metals and Carbon Materials: A Brief Review", *Frontiers in Chemistry*, **8**, 552 (2020).

[2] V. L. STOUT, M. D. GIBBONS, "Gettering of Gas by Titanium", *Journal of Applied Physics*, **26**, 1488 (1955).

[3] S. KUMAR et al., "Development of Vanadium Based Hydrogen Storage Material: A Review", *Renewable and Sustainable Energy Reviews*, **72**, 791–800 (2017).

[4] S. P. GARG, E. A. GULBRANSEN, P. VIJENDRAN, "Zr Powder and Zr-16% Al Alloy as Getters for O_2, H_2, H_2O, CO and CO_2 Gases", *Vacuum*, **40**, 275–280 (1990).

[5] K. GOTO et a., "Suitability Evaluation of $LaNi_5$ as Hydrogen-Storage-Alloy Actuator by In-Situ Displacement Measurement During Hydrogen Pressure Change", *Molecules*, **24**, 2420 (2019).

[6] K. JUNG et al., "Performance of a Depleted Uranium Bed for a Nuclear Fusion Fuel Cycle", *Fusion Science and Technology*, **71**, 416–421 (2017).

[7] M. T. BRUMBACH et al., "Activation of Erbium Films for Hydrogen Storage", *Journal of Applied Physics*, **109**, 114911 (2011).

[8] I. GABIS et al., "Kinetics of Decomposition of Erbium Hydride", *Journal of Alloys and Compounds*, **356-357**, 353–357 (2003).

[9] H. ZHOU et al., “Effect of Pre-Damage Induced by Argon Ions on the Following 60 keV Helium Ions Irradiation Behavior of Tungsten-Tantalum Alloy”, *Fusion Engineering and Design*, **154**, 111533 (2020).

[10] H. Y. CHEN et al., “The Influence of Different Isochronal Annealing Temperature on Helium Ion Irradiation Damage of W-Nb Composites”, *Fusion Engineering and Design*, **159**, 111857 (2020).

[11] Y. SUO et al., “Study on the Irradiation Damage in Fe-Based Metallic Glasses Induced by Ne10+ Ions”, *Fusion Engineering and Design*, **157**, 111635 (2020).

[12] M. SHIMADA et al., “Overview of the US-Japan Collaborative Investigation on Hydrogen Isotope Retention in Neutron-Irradiated and Ion-Damaged Tungsten”, *Fusion Engineering and Design*, **87**, 1166–1170 (2012).

[13] H. T. LEE et al., “Incident Ion Energy and Temperature Dependence of Helium Bubble Formation and its Impact on D-Retention Under Simultaneous He-D Irradiation of Tungsten”, *Fusion Science and Technology*, **63**, 233–236 (2013).

[14] S. KONDO et al., “High Temperature Ion-Irradiation Effects on Microstructural Evolution in β-SiC”, *Fusion Science and Technology*, **44**, 181–185 (2003).

[15] N. YOSHIDA et al., “Damage and Deuterium Retention of Beryllium due to Low Energy Deuterium Ion Irradiation”, *Fusion Science and Technology*, **30**, 798–801 (1996).

[16] Y. LIU et al., “Hydrogenation of Zirconium Film by Implantation of Hydrogen Ions”, *Plasma Science and Technology*, **19**, 035502 (2019).

[17] A. Y. DIDYK et al., “Depth Concentrations of Deuterium Ions Implanted into Some Pure Metals and Alloys”, *Physics of Particles and Nuclei Letters*, **9**, 86–95 (2012).

[18] B. PANIGRAHI, K. G. M. NAIR, K. KRISHAN, “Study of Deuterium Metal Interaction by ion Implantation”, *Bulletin of Materials Science*, **19**, 61–72 (1996).

[19] A. LÓPEZ-SUÁREZ, “Improvement of Hydrogen Absorption in Ti Induced by Ion Irradiation”, *Nuclear Instruments and Methods in Physics Research Section B: Beam Interactions with Materials and Atoms*, **B436**, 198–202 (2018).

[20] H. KOSTLER et al., “A New Hydride: MgHx Prepared by Ion Implantation”, *Journal of Physics: Condensed Matter*, **3**, 8767–8776 (1991).

[21] A. MANHARD et al, “Deuterium implanted into polycrystalline tungsten: Novel TPD investigation”, presented at 13th International Workshop on Plasma-Facing Materials and Components for Fusion Applications, Rosenheim, (2011).

[22] H. ABE et al., “Improvement of Hydrogen Absorption Rate of Pd by Ion Irradiation”, *Nuclear Instruments and Methods in Physics Research Section B: Beam Interactions with Materials and Atoms*, **B206**, 224–227 (2003).

[23] H. BERNAS, A. TRAVERSE, “Atomic Displacements in Metals due to Low-Energy Light Ion Implantation”, *Applied Physics Letters*, **41**, 245 (1982).

[24] A. HOLLINGSWORTH et al., “Comparative Study of Deuterium Retention in Irradiated Eurofer and Fe-Cr from a New Ion Implantation Materials Facility”, *Nuclear Fusion*, **60**, 016024 (2020).

[25] J. MULLER, B. SINGH, N. A. SURPLICE, “The Gettering Action of Evaporated Films of Titanium and Erbium”, *Journal of Physics D - Applied Physics*, **5**, 1177–1184 (1972).

[26] P. M. S. JONES, P. ELLIS, T. ASLETT, “Thermal Stability of Metal Hydrides, Deuterides and Tritides”, *Nature*, **223**, 829–830 (1969).

[27] H. H. SHEN et al., “Influencing Factors of Helium Bubble Growth in Erbium Tritides: Grain Size and Impurity Element”, *Journal of Alloys and Compounds*, **860**, 157911 (2021).

[28] J. L. PROVO, “Effect of Vacuum Processing Erbium Dideuteride/Ditritide Films Deposited on Chromium Underlays on Copper Substrates”, *Journal of Vacuum Science and Technology*, **16**, 230 (1979).

[29] R. M. FERRIZZ, “Erbium Hydride Thermal Desorption: Controlling kinetics”, SAND2007-2659, Sandia National Laboratories, (2007).

[30] A. MANHARD, T. SCHWARZ-SELLINGER, W. JACOB, “Quantification of the Deuterium Ion Fluxes from a Plasma Source”, *Plasma Sources Science and Technology*, **20**, 015010 (2011).

[31] S. H. KING, C. R. TEWELL, “Metastable erbium trihydrides supported films and powders, presented at Hydrogen and Helium Isotopes in Materials”, Albuquerque, New Mexico, (2005).

[32] S. SUWARNO, M. V. LOTOTSKYY, V. A. YARTYS, “Thermal Desorption Spectroscopy Studies of Hydrogen Desorption from Rare Earth Metal Trihydrides REH_3 (RE=Dy, Ho, Er)”, *Journal of Alloys and Compounds*, **842**, 155530 (2020).

[33] R. M. FERRIZZ, “Erbium hydride decomposition kinetics”, SAND2006-7014, Sandia National Laboratories, (2006).

[34] R. FERRIZZ et al, “PCT study: Erbium-hydrogen system (preliminary results), presented at Hydrogen and Helium Isotopes in Materials Conference, Albuquerque, New Mexico, (2008).

[35] M. A. RODRIGUEZ et al., “In Situ Observation of ErD_2 Formation During D_2 Loading via Neutron Diffraction”, *Powder Diffraction*, **26**, 144–148 (2011).

[36] W. MAO et al., “Hydrogen Isotope in Erbium Oxide: Adsorption, Penetration, Diffusion and Vacancy Trapping”, *Fusion Engineering and Design*, **95**, 35–40 (2015).

[37] J. F. ZIEGLER, M. D. ZIEGLER, J. P. BIERSACK, “SRIM – The Stopping and Range of Ions in Matter”, *Nuclear Instruments and Methods in Physics Research Section B: Beam Interactions with Materials and Atoms*, **B268**, 1818–1823 (2010)